BULLETIN OF THE EARTHQUAKE
RESEARCH INSTITUTE
Vol. 45 (1967), pp. 997-1018

51. *Long Waves Invading Obliquely to a Semi-circular Peninsula.*

By Takao MOMOI,

Earthquake Research Institute.

(Read September 12, 1967.—Received September 23, 1967.)

Abstract

In the present work, the coastal response of a semi-circular peninsula for the oblique (45 degree) invasion of a train of periodic waves is treated. Numerical calculation of *RST* (resultant) waves, *RD* (reflected and diffracted) waves and *SC* (scattered) waves were carried out for a few numbers of the periods of waves. One of the most conspicuous features obtained in the present work is a generation of the standing waves along the coast of the peninsula.

1. Introduction

In the previous papers[1),2)] entitled "Diffraction of Tsunami Invading a Semi-circular Peninsula" and "A Further Study of Diffraction of Tsunami Invading a Semi-circular Peninsula", long waves invading a peninsula perpendicular to the straight coast are treated. In this study, long waves around a semi-circular peninsula are discussed for the case where a train of periodic waves invades the peninsula at an angle of 45 degrees to the straight coast.

2. Theory

Referring to Fig. 1, the polar coordinates (r, θ) are centered at the midpoint of the semicircle of the peninsula, the basal line $(\theta=0)$ being taken along the straight coast. The radius of the peninsula is r_0.

Let ζ and k be respectively the wave height and the wave number of the incident waves. The equation for periodic waves is then

1) T. MOMOI, *Bull. Earthq. Res. Inst.*, **41** (1963), 589-594.
2) T. MOMOI, *Bull. Earthq. Res. Inst.*, **44** (1966), 473-480.

$$\left(\frac{\partial^2}{\partial r^2}+\frac{1}{r}\frac{\partial}{\partial r}+\frac{1}{r^2}\frac{\partial^2}{\partial\theta^2}+k^2\right)\zeta=0\,. \tag{1}$$

The boundary conditions are

$$\frac{1}{r}\frac{\partial\zeta}{\partial\theta}=0 \quad (\theta=0 \text{ and } \pi\,;\ r>r_0) \tag{2}$$

at the straight coast, and

$$\frac{\partial\zeta}{\partial r}=0 \quad (r=r_0\,;\ 0<\theta<\pi) \tag{3}$$

at the coast of the peninsula.

When a train of periodic waves is propagated to the coast with an inclination of θ_{in} radians to the straight coast, it is expressed as

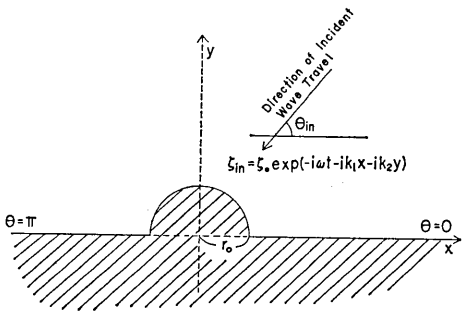

Fig. 1. Geometry of the model used.

$$\zeta_{in}=\zeta_0\exp\{-ikr\cos(\theta-\theta_{in})\}\,, \tag{4}$$

where ζ_{in} and ζ_0 are respectively the wave height and amplitude of the incident waves. The time factor $\exp(-i\omega t)$ is omitted as usual (ω: the angular frequency of the incident waves), unless otherwise stated.

A general solution of the equation (1) is described as

$$\zeta=\zeta_{in}+\zeta_r^{(p)}+\zeta_{sc}\,, \tag{5}$$

where

ζ_{in}: the incident wave given by (4);

$\zeta_r^{(p)}$: a particular solution of (1) which satisfies the boundary condition (2), having the nature of reflected waves;

ζ_{sc}: scattered waves having the nature of outgoing waves at an infinite point.

As a particular solution, we can take a form

$$\zeta_r^{(p)}=\zeta_0\exp\{-ikr\cos(\theta+\theta_{in})\}\,, \tag{6}$$

which satisfies the equation (1). The expression (6) also satisfies the condition (2) together with the incident wave ζ_{in}.

Now if one obtains a (general) solution ζ_{sc} denoting the scattered waves around the peninsula, a desired solution ζ is given by (5).

Assuming that the scattered waves are axisymmetric with respect to the straight coast, they are described by the series ($\zeta^{(m)}$: unknowns)

$$\zeta_{sc}=\sum_{m=0}^{\infty}\zeta^{(m)}H_m^{(1)}(kr)\cos m\theta\,. \tag{7}$$

The above expression satisfies the boundary condition (2).

Using the formula

$$\exp(i\cdot z\cos\theta)=\sum_{n=0}^{\infty}\varepsilon_n(-1)^nJ_{2n}(z)\cos 2n\theta + i\cdot 2\sum_{n=0}^{\infty}(-1)^nJ_{2n+1}(z)\cos(2n+1)\theta\,, \tag{8}$$

the sum of ζ_{in} and $\zeta_r^{(p)}$ is reduced, after a few algebraic manipulations, to the following.

$$\zeta_{in}+\zeta_r^{(p)}=2\zeta_0\sum_{n=0}^{\infty}\varepsilon_n(-1)^nJ_{2n}(kr)\cos 2n\theta_{in}\cos 2n\theta - i\cdot 4\zeta_0\sum_{n=0}^{\infty}(-1)^nJ_{2n+1}(kr)\cos(2n+1)\theta_{in}\cos(2n+1)\theta\,, \tag{9}$$

where

$$\varepsilon_0=1 \quad\text{and}\quad \varepsilon_n=2\ (n\geqq 1)\,.$$

In order to determine the unknown factors $\zeta^{(m)}$, the boundary condition (3) at the coast of the peninsula is used. Substituting (5) with the expressions (7) and (9) into (3), we have

$$2\zeta_0\sum_{n=0}^{\infty}\varepsilon_n(-1)^nJ'_{2n}(kr_0)\cos 2n\theta_{in}\cos 2n\theta - i\cdot 4\zeta_0\sum_{n=0}^{\infty}(-1)^nJ'_{2n+1}(kr_0)\cos(2n+1)\theta_{in}\cos(2n+1)\theta + \sum_{m=0}^{\infty}\zeta^{(m)}H_m^{(1)\prime}(kr_0)\cos m\theta=0\,. \tag{10}$$

Applying the operators

$$\int_0^{\pi}\cos m\theta d\theta \quad (m=0,1,2,\cdots)$$

to (10), the relation (10) is reduced to

$$\left.\begin{aligned}&\zeta^{(2n)}=(-1)^{n+1}\cdot 2\zeta_0\varepsilon_n\cos 2n\theta_{in}J'_{2n}(kr_0)/H^{(1)\prime}_{2n}(kr_0)\\ \text{and}\qquad&\\ &\zeta^{(2n+1)}=i\cdot(-1)^n\cdot 4\zeta_0\cos(2n+1)\theta_{in}J'_{2n+1}(kr_0)/H^{(1)\prime}_{2n+1}(kr_0)\ ,\end{aligned}\right\}\qquad(11)$$

where $n=0, 1, 2, \cdots$.

Now if one uses an electronic computer, the height and phase of the waves are readily computed through (5) with the expressions (7), (9) and (11).

For convenience of later discussions, the components of the waves are named in the following ways.

RST waves: the waves described by (5) (*RST* waves are the abbreviations of resultant waves),

RD waves : the waves composed of the last two of (5), i.e. $\zeta_r^{(p)}+\zeta_{sc}$ (*RD* is the abbreviation of "reflected and diffracted"), which are purely reflected and diffracted waves excluding the incident ones from *RST* waves,

SC waves : the scattered waves expressed by (7) (*SC* is the abbreviation of "scattered"). The scattered waves are the modification components due to the existence of a peninsula upon the waves which are produced at a straight coast.

Numerical calculations are carried out for the waves of long wavelengths, i.e. $kr_0=0.5$, 1.0 and 2.0, and for an incidence angle $\theta_{in}=45$ degrees. In the subsequent sections, the results of the numerical calculations are discussed.

3. *RST* Waves

In this section, the discussion of *RST* waves (resultant waves) expressed by (5) is made. The variations of the amplitude of *RST* waves are presented in Figs. 2a (for $kr_0=0.5$), 3a (for $kr_0=1.0$) and 4a (for $kr_0=2.0$), while those of the phase are shown in Figs. 2p ($kr_0=0.5$), 3p ($kr_0=1.0$) and 4p ($kr_0=2.0$). The values of the amplitude and phase are calculated by $|\zeta|$ and $\arg\zeta$ based on the expression (5). The computed values of $\arg\zeta$ are taken in the range of the principal value of the tangent.

According to Figs. 2a, 3a and 4a, a region of high amplitude appears in the windward side of the semi-circular peninsula, which is interpreted

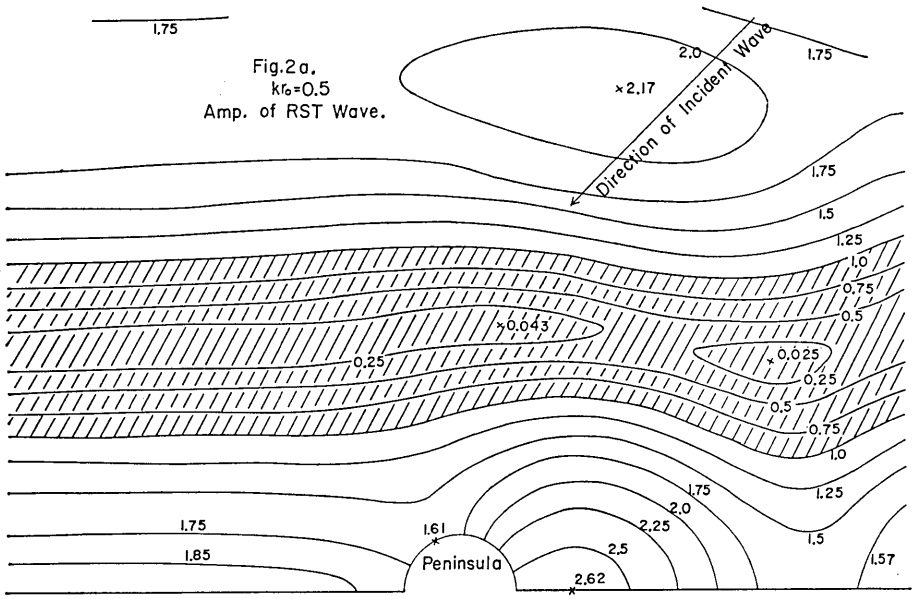

Fig. 2a. Variation of the amplitude of *RST* wave for $kr_0=0.5$. The stated numerals in the figure denote the values of $|\zeta|$ which are normalized by the amplitude of the incident wave. This convention is followed in the following Figs. 3a and 4a.

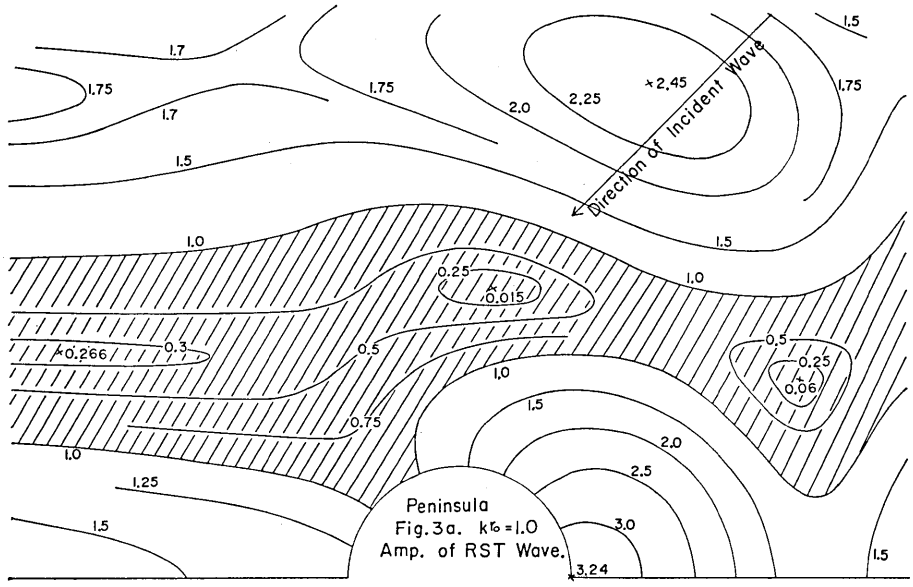

Fig. 3a. Variation of the amplitude of *RST* wave for $kr_0=1.0$.

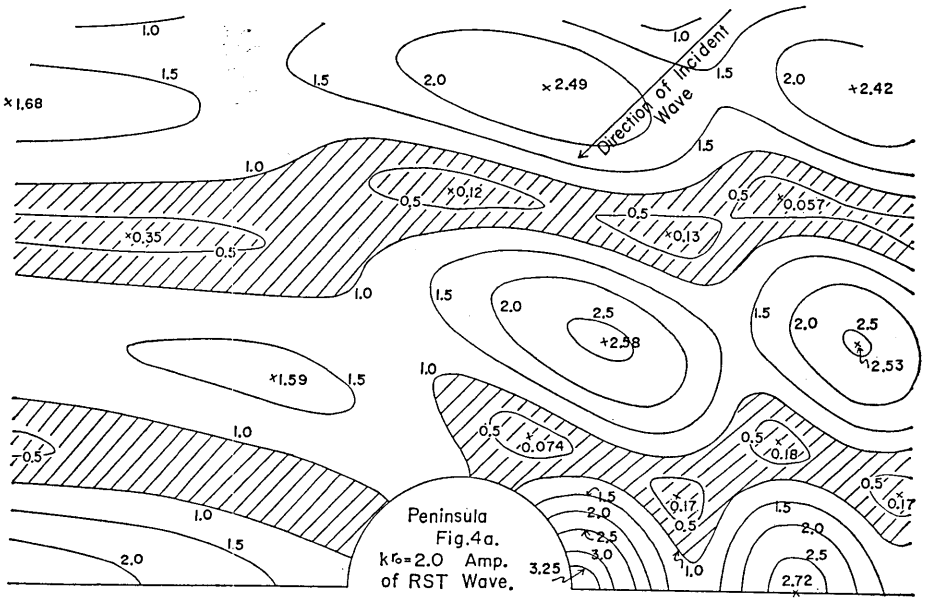

Fig. 4a. Variation of the amplitude of RST wave for $kr_0=2.0$.

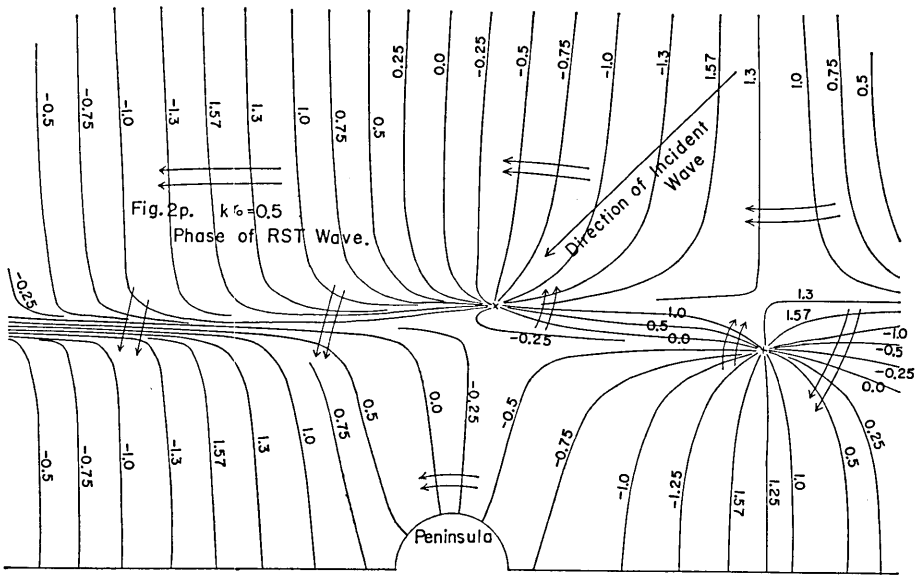

Fig. 2p. Variation of the phase of RST wave for $kr_0=0.5$. The stated numerals in the figure denote the values of $\arg\zeta$ which are calculated in the range of the principal value of the tangent, i.e. $-\pi/2<\arg\zeta\leqq\pi/2$. This convention is followed in Figs. 3p and 4p.

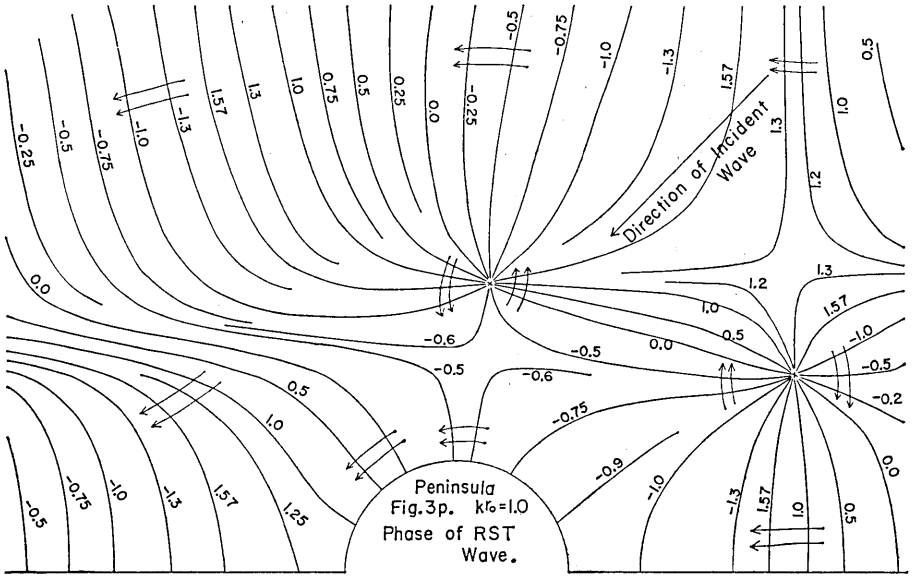

Fig. 3p. Variation of the phase of *RST* wave for $kr_0=1.0$.

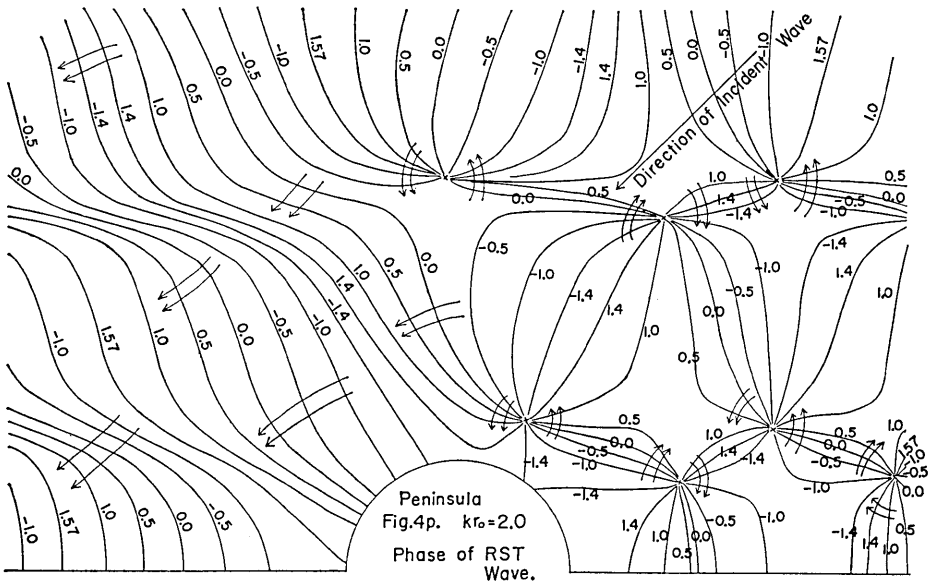

Fig. 4p. Variation of the phase of *RST* wave for $kr_0=2.0$.

as being a result of the trapping of the incident waves in this area of water (see Fig. 5).

If there is no obstacle along the straight coast, standing waves appear in front of the coast which are moving parallel to the coast. That is to say, when there is no obstacle, the expression of the wave height becomes as follows, from (5):

$$\zeta=\zeta_0 \exp\{-ikr\cos(\theta-\theta_{in})\} +\zeta_0 \exp\{-ikr\cos(\theta+\theta_{in})\}\ .$$

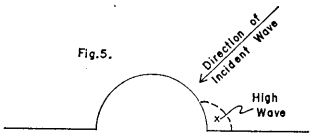

Fig. 5. Generation of high waves.

Transforming the above expression, we have

$$\zeta=2\zeta_0 \cos k_2 y\cdot e^{-ik_1 x}\ , \qquad (12)$$

where

$$\left.\begin{aligned} k_1&=k\cos\theta_{in}\\ k_2&=k\sin\theta_{in}\end{aligned}\right\}\text{, i.e., components of wave number vector}$$

and

$$\left.\begin{aligned} x&=r\cos\theta\\ y&=r\sin\theta\end{aligned}\right\}\text{, i.e., components of cartesian coordinates.}$$

The expression (12) reveals that standing waves, which move parallel to the coast, are produced in front of a straight coast.

When the parameter kr_0 is small (which is referred to the waves of long wave-length as compared with the radius of the semi-circular peninsula), the modification of the standing waves (described in (12)) due to the peninsula is small (refer to Fig. 2a), whereas when kr_0 begins to be large (see Figs. 3a and 4a), the modification becomes large also, as would be expected.

In Figs. 2a to 4a, regions with the amplitude below 1.0 are shaded. From the above shaded patterns in the nearby waters of the peninsula, a very interesting penomenon is found such that standing waves are produced along the coast of the semi-circular peninsula. That is to say, if the length of the periphery of the semi-circular peninsula is reduced to that of a one-dimensional tank (refer to Fig. 6), motions of water along the coast of the peninsula for specified parameters $kr_0=1.0$ and 2.0 correspond respectively to the first and second modes of motions of water in the one-dimensional tank. As figuratively shown in Fig. 6, the

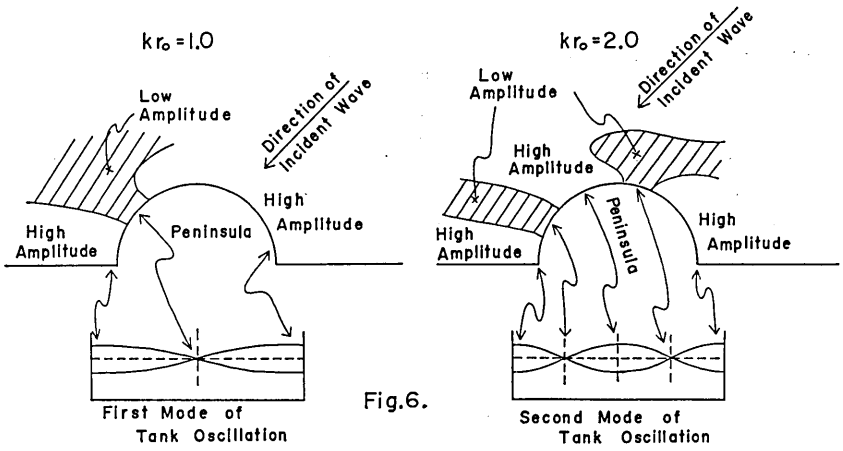

Fig. 6. Correspondence of the waves along the coast of the peninsula and the motion of water in a rectangular tank.

low and high parts of the amplitude along the coast of the peninsula are referred to the nodes and loops of the tank oscillation. In Fig. 2a, the above-mentioned standing mode does not appear, since the parameter $kr_0=0.5$ does not correspond to a resonant mode.

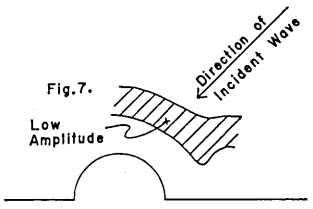

Fig. 7. Circular extension of the low-amplitude part.

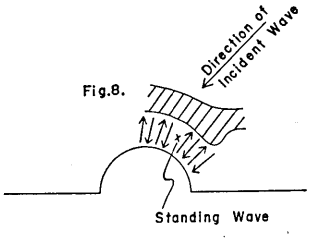

Fig. 8. Generation of radial standing waves.

Throughout three figures (Figs. 2a to 4a), areas of smaller amplitude extend relatively in circular form in the windward side of the peninsula (see Fig. 7), though the zones of the above areas run discontinuously in Fig. 4a. The above circular extension of the variation of the amplitude is considered as being produced by the standing waves which might be generated in the windward side of the peninsula (see Fig. 8). In order to ascertain such a possibility, the nodal lines, which are calculated by

$$\cos k(r-r_0)=0 \tag{13}$$

are described in Fig. 9 only for the case of $kr_0=2.0$. The calculation of the node by (13) is a little dubious for a two-dimensional problem such as the present case, but use of equation (13) might be permissible as a first approximation. In Fig. 9, regions of low amplitude (below 1.0) are also described by shaded parts. Fig. 9 reveals that regions of low amplitude extend approximately along the nodal lines depicted based on the equation (13).

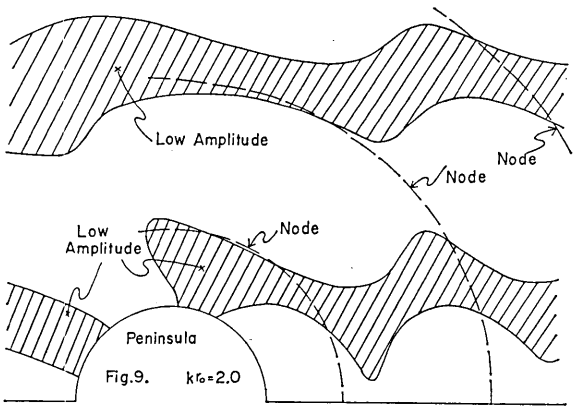

Fig. 9. Nodal lines calculated by $\cos k(r-r_0)$ for the case of $kr_0=2.0$.

Through three figures (Figs. 2a to 4a), variations of the amplitude in the windward side of the peninsula are greater than those in the leeward side (see Fig. 10). The violence of the former is interpreted as being caused as a result of a generation of reflected waves in the windward part of the peninsula.

Next, let us discuss the variation of phase.

When there is no projection in a straight coast, the waves stationary in the y-direction (perpendicular to the coast) move to the negative side of x (parallel to the coast), as already shown in (12). The crestlines showing the variation of phase then must run perpendicular to the straight coast. When the above projection is small (the case for $kr_0=$ 0.5, i.e., Fig. 2p), the modification of the above crestlines is slight, while the modification becomes so great with a decrease in wave-length of the incident waves compared to a dimension of the peninsula (refer

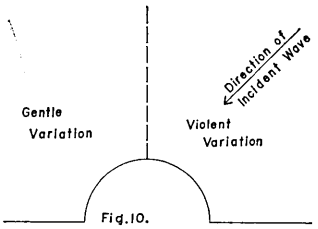

Fig. 10. Spatial distribution of the variations of the amplitude.

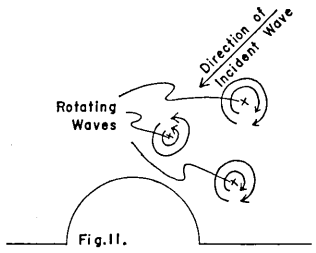

Fig. 11. Appearance of the rotating waves.

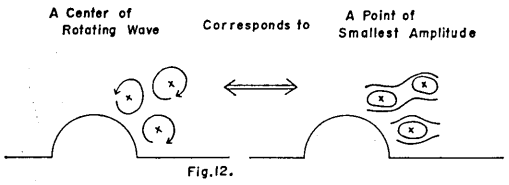

Fig. 12. Agreement of the center of the rotating waves and the point of the lowest amplitude.

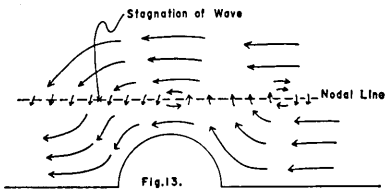

Fig. 13. Appearance of the stagnation line of waves.

to Figs. 3p and 4p) that the original form of the crestlines described by (12) disappears for the case $kr_0=2.0$ (Fig. 4p).

Three figures concerning the variation of phase (Figs. 2p to 4p) show us an appearance of rotating waves in the windward waters of the peninsula (see Fig. 11). Comparing Figs. 2p, 3p and 4p with Figs. 2a, 3a and 4a respectively, it turns out that a center of the rotating waves corresponds to a point of smallest amplitude (see Fig. 12).

In Figs. 2p to 4p, the waves stagnate along the nodal line expressed by (12) (refer to Fig. 13).

4. *RD* Waves

In this section, *RD* waves $(\zeta_r^{(p)}+\zeta_{sc})$ expressed by (6) and (7) are discussed. The results of the calculations are presented respectively in Figs. 14a, 15a and 16a for the variations of the amplitude of $kr_0=0.5$, 1.0 and 2.0, while the variations of the phase are shown respectively in Figs. 14p, 15p and 16p for $kr_0=0.5$, 1.0 and 2.0. The amplitude and phase of *RD* waves are computed by $|\zeta_{rd}|$ and arg ζ_{rd}, where the computed values of arg ζ_{rd} are taken in the range of the principal value of the tangent.

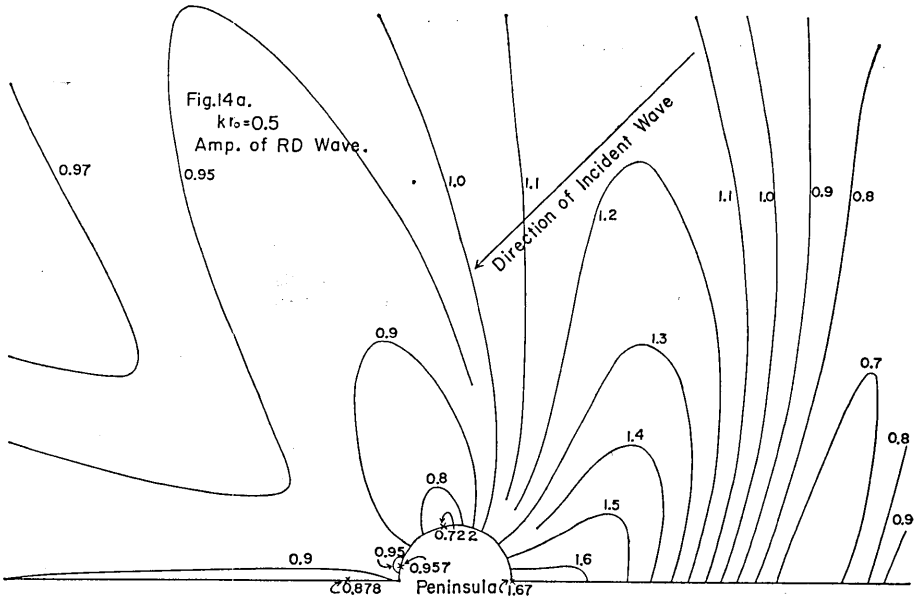

Fig. 14a. Variation of the amplitude of *RD* wave for $kr_0=0.5$. The stated numerals in the figure denote the values of $|\zeta_{rd}|$ which are normalized by the amplitude of the incident wave. This convention is followed in the following Figs. 15a and 16a.

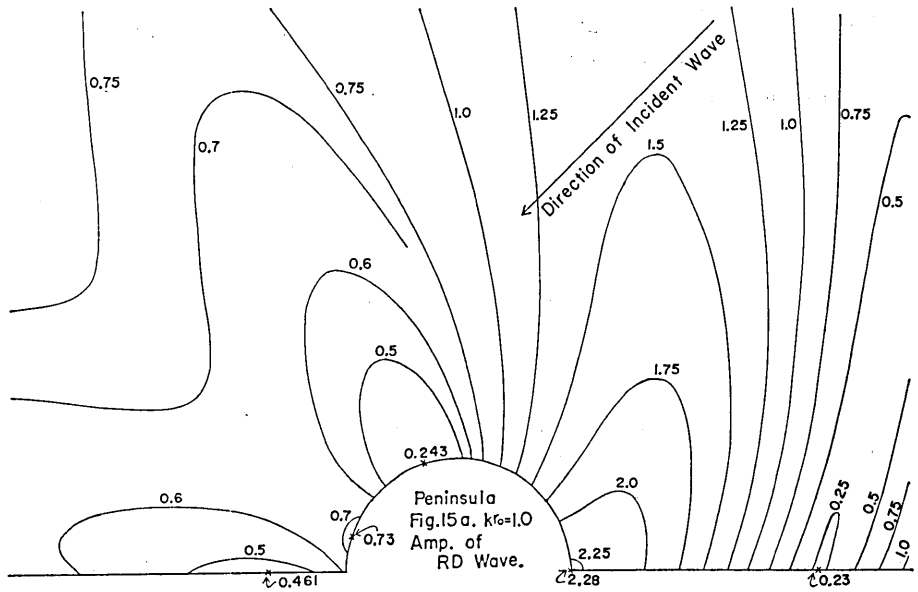

Fig. 15a. Variation of the amplitude of *RD* wave for $kr_0=1.0$.

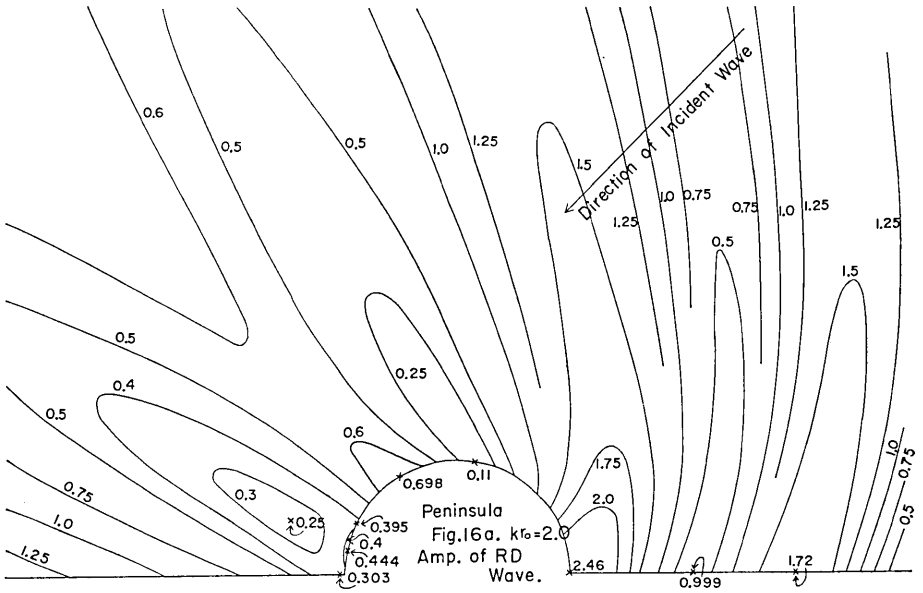

Fig. 16a. Variation of the amplitude of *RD* wave for $kr_0=2.0$.

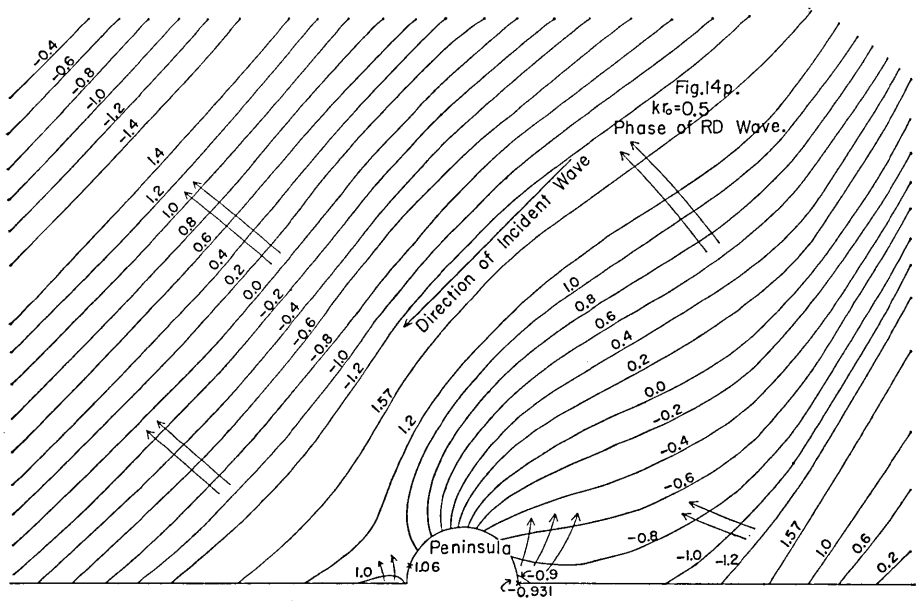

Fig. 14p. Variation of the phase of *RD* wave for $kr_0=0.5$. The stated numerals in the figure denote the values of $\arg \zeta_{rd}$ which are calculated in the range of the principal value of the tangent. This convention is followed in Figs. 15p and 16p.

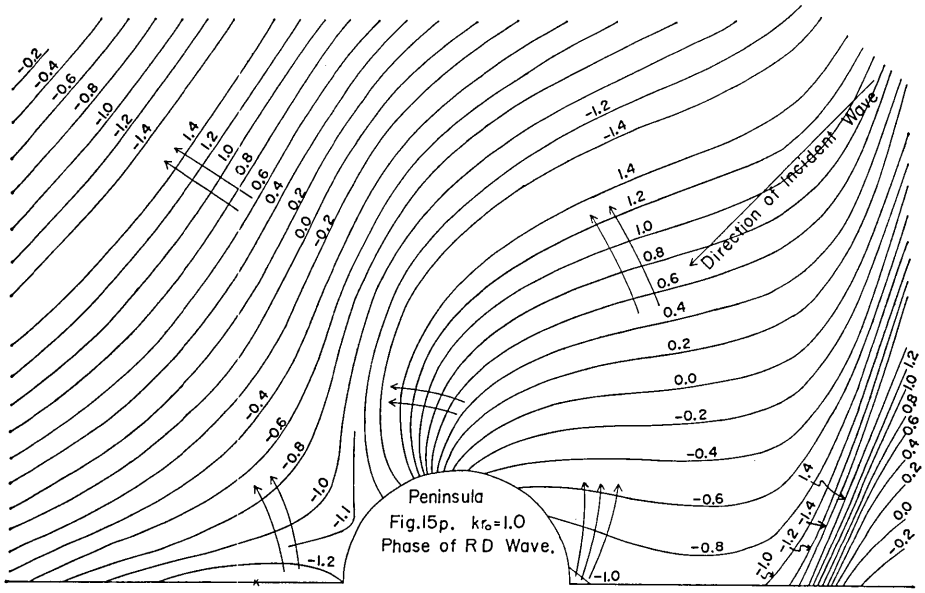

Fig. 15p. Variation of the phase of *RD* wave for $kr_0=1.0$.

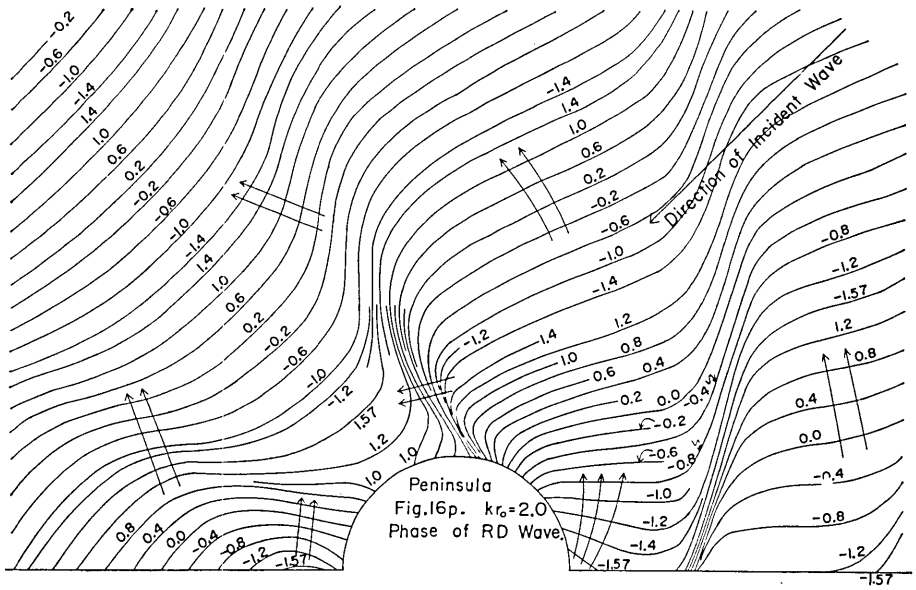

Fig. 16p. Variation of the phase of *RD* wave for $kr_0=2.0$.

Referring to Figs. 14a to 16a, a region of large amplitude extends from the windward side of the roots of the peninsula to the outer sea (see Fig. 17). Such highness of the amplitude is considered as being caused by the emission of waves trapped in this part of waters. On the leeward side of the above high amplitude region, an area of relatively lower amplitude also extends from the coast of the peninsula to the outer sea (Fig. 17). As will be shown in Figs. 14p to 16p, this area of lower amplitude corresponds to the geometric shadow of *RD* waves emitted from the root of the peninsula (refer to Fig. 18).

As far as the phase variation of *RD* waves is concerned, the following facts are exposed (referring to Figs. 14p, 15p and 16p). Through three figures, a conspicuous feature is the emission of two types of waves. One is the emission of the trapped waves from the windward side of the peninsula, while the other is the emission (reflection) of the waves (diffrated along the coast of the peninsula) from the leeward side of the root (refer to Fig. 19). When the wave-length of the incident

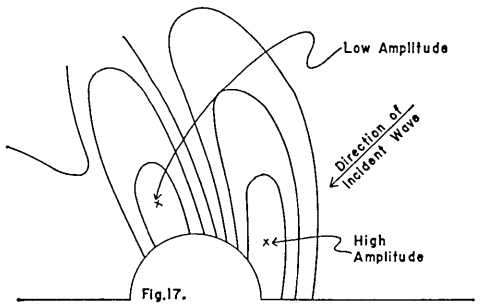

Fig. 17. Extension of high waves from the windward side of the roots of the peninsula.

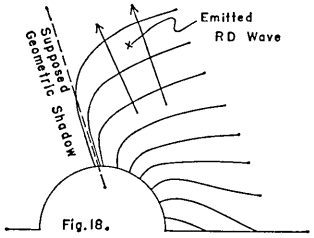

Fig. 18. Appearance of the geometric shadow of *RD* wave.

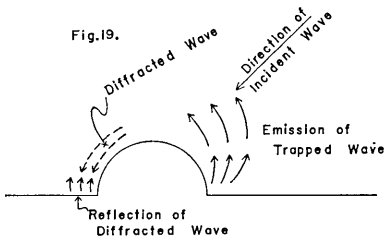

Fig. 19. Emissions of two types of waves.

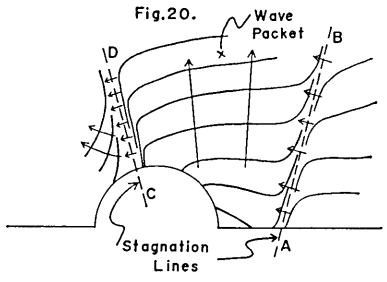

Fig. 20. Generation of the wave packet.

waves becomes small as compared with the radius of the peninsula, say the case of Fig. 16p ($kr_0=2.0$), directivity of the waves begins to be so great that a packet of reflected waves is generated in the windward part of the peninsula being held between two stagnation lines of waves (lines stated by AB and CD in Fig. 20). Leaving from the coast, the above stagnation lines gradually become obscure as a result of the divergence of the waves.

5. SC Waves

In this section, the variations of SC waves (ζ_{sc}) described in (7) are considered. The calculated results are shown in Figs. 21a, 22a and 23a for the amplitude variations of $kr_0=0.5$, 1.0 and 2.0, while the phase variations are presented respectively in Figs. 21p, 22p and 23p for $kr_0=$ 0.5, 1.0 and 2.0. The amplitude and phase are calculated by $|\zeta_{sc}|$ and $\arg\zeta_{sc}$, the latter of which is taken in the range of the principal value of the tangent.

Referring to Figs. 21a to 23a and 21p to 23p, the following facts are exposed.

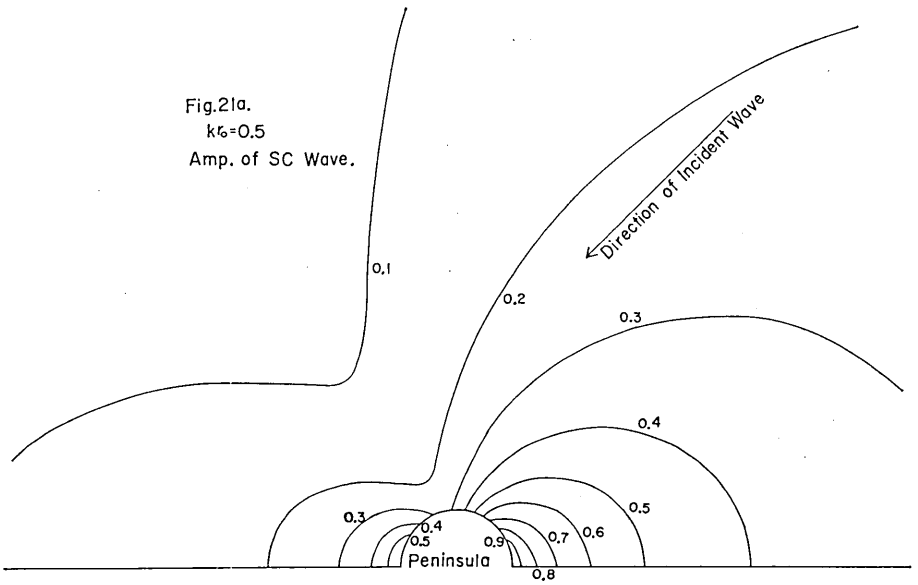

Fig. 21a. Variation of the amplitude of SC wave for $kr_0=0.5$. The numerals stated in the figure denote the values of $|\zeta_{sc}|$ which are normalized by the amplitude of the incident wave. This convention is followed in Figs. 22a and 23a.

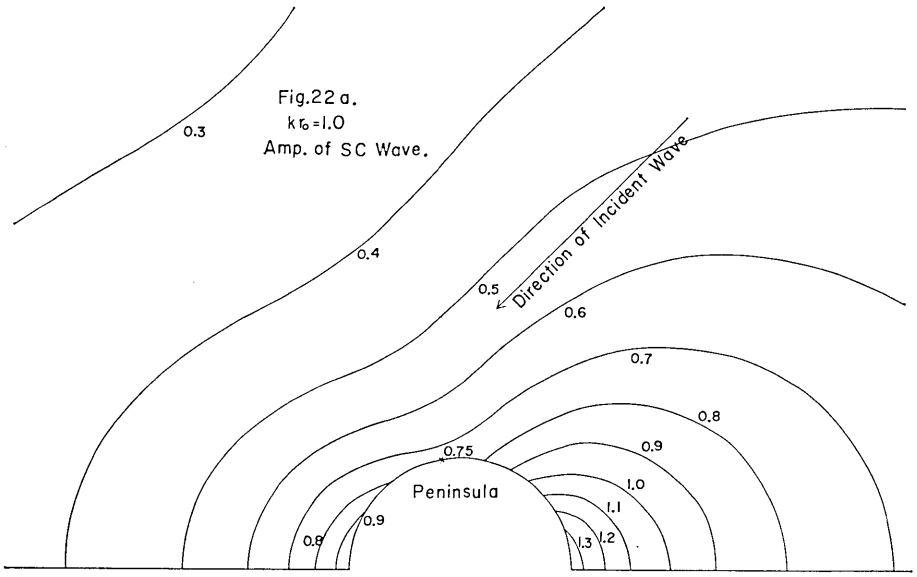

Fig. 22a. Variation of the amplitude of *SC* wave for $kr_0=1.0$.

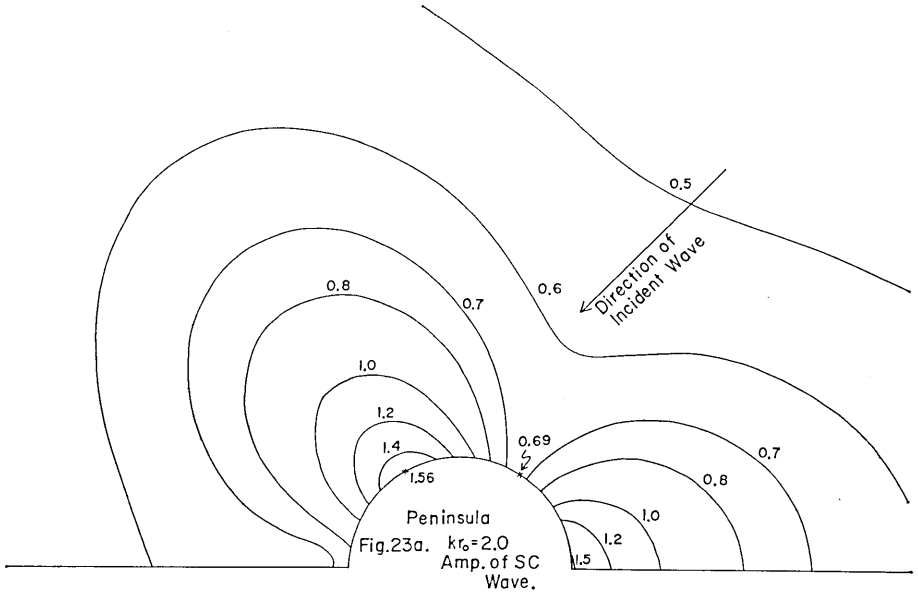

Fig. 23a. Variation of the amplitude of *SC* wave for $kr_0=2.0$.

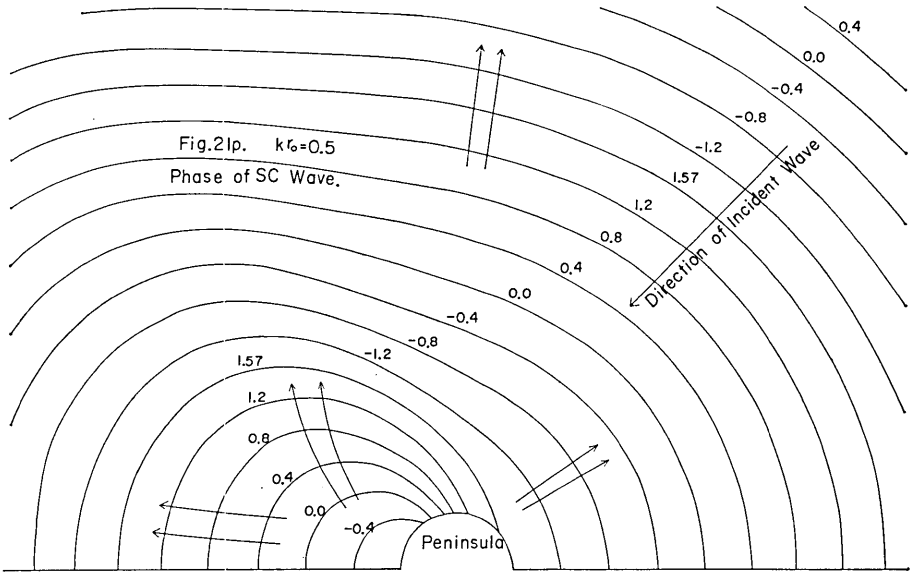

Fig. 21p. Variation of the phase of *SC* wave for $kr_0=0.5$. The numerals stated in the figure denote the values of $\arg \zeta_{sc}$ which are calculated in the range of the principal value of the tangent. This convention is used in the following two figures, i.e., Figs. 22p and 23p.

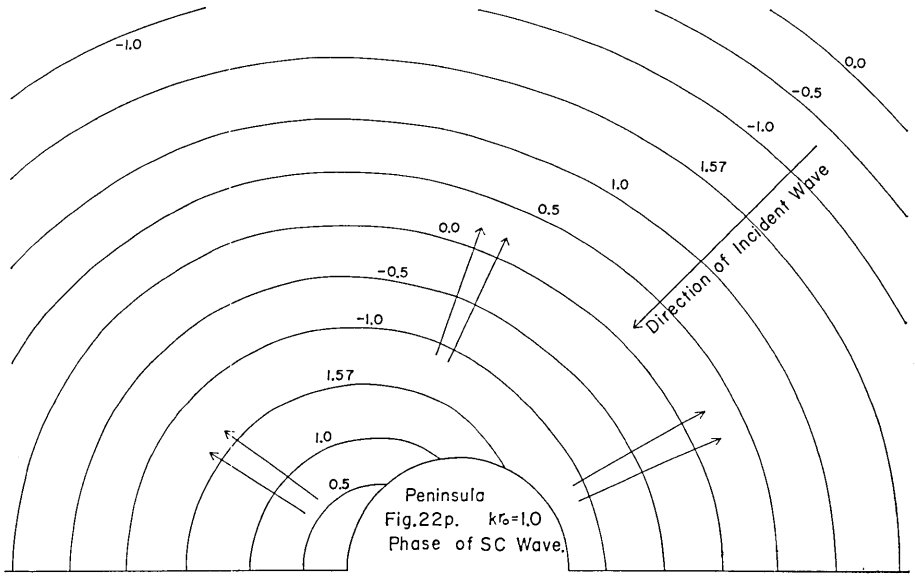

Fig. 22p. Variation of the phase of *SC* wave for $kr_0=1.0$.

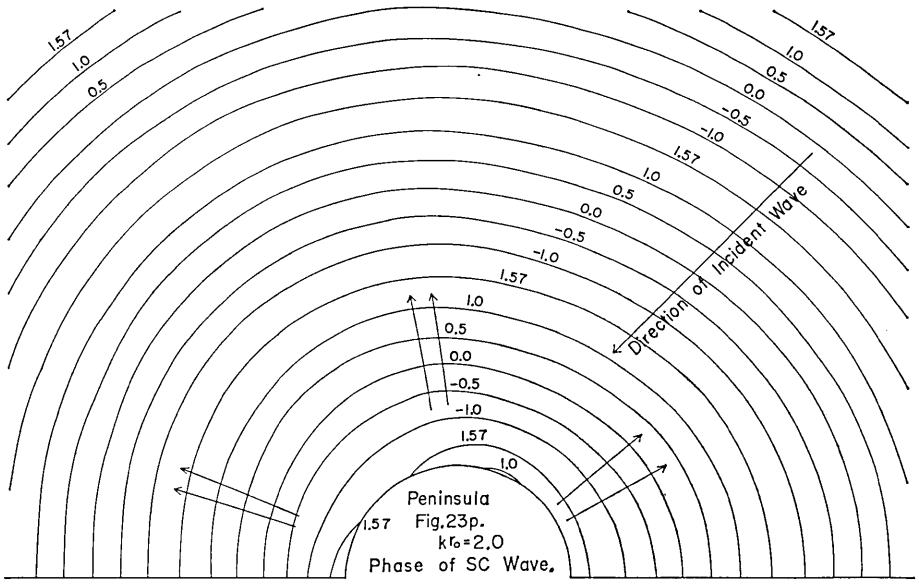

Fig. 23p. Variation of the phase of *SC* wave for $kr_0=2.0$.

From the above six figures, a strong emission of scattered waves from the nearby part of the windward side root of a peninsula is found.

Passing through the three figures relevant to the amplitude of *SC* waves (Figs. 21a to 23a), when kr_0 is small (which corresponds to the case of waves of long wave-length as compared with the radius of the peninsula), a region of large amplitude appears in the nearby waters of the leeward-side root of the peninsula (refer to Fig. 21a), which, as kr_0 increases (referring to Figs. 22a and 23a), this region of high waves gradually disappears. Such a generation of large amplitudes for *small* kr_0 is interpreted as being caused by the result of the strong diffraction of waves of longer wave-length on the leeward waters of the peninsula (refer to Fig. 24).

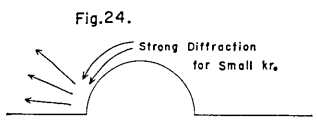

Fig. 24. Strong inflow to the leeward waters of the peninsula for small kr_0.

A similar phenomenon is shown in the work[3] entitled "Long Waves around a Circular Island [I]", where a definite explanation was not given on the above problem. That is to say, referring to Figs. 5 and 9 in the above-mentioned work[3] (which are relevant to the phase variations of scattered waves around an island for

3) T. Momoi, *Bull. Earthq. Res. Inst.*, **44** (1967), 347-359.

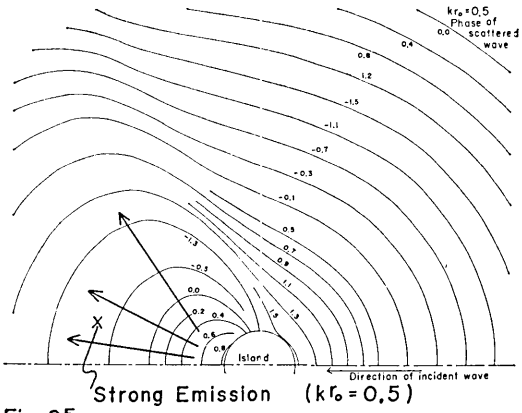

Fig.25.

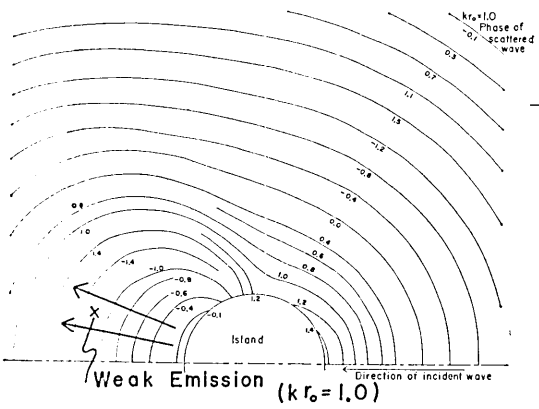

Fig. 25. Scattered waves around an island.

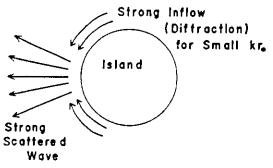

Fig.26.

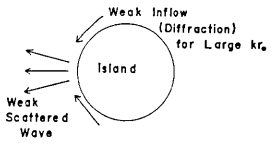

Fig. 26. Figurative explanation of the behavior of the scattered waves.

Fig.27.

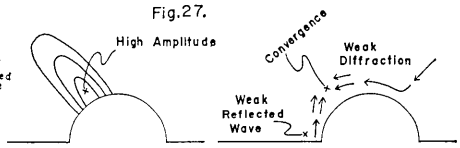

Fig. 27. Generation of the high-amplitude region for large kr_0.

Fig.28.

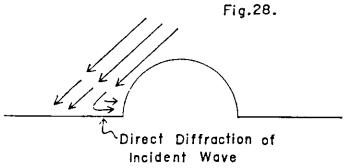

Fig. 28. Generation mechanism of week reflected waves in the leeward waters.

the parameters kr_0=0.5 and 1.0 respectively), the emission of waves of longer wave-length (kr_0=0.5) from the leeward coast of the island is found more definitely than for waves of relatively shorter wave-length (kr_0=1.0). These figures for the island are reproduced in Fig. 25. A physical interpretation for this phenomenon is that a stronger inflow of the invading waves to the leeward waters of the island for small kr_0 causes a stronger emission of scattered waves from the leeward coast, while weaker inflow of the invading waves for relatively larger kr_0 results in weaker emission of scattered waves (refer to Fig. 26).

In Fig. 23a (for kr_0=2.0), a peculiar extension of the large amplitude

region from the coast of the peninsula to the outer sea is found in the leeward waters (refer to the left-hand side figure of Fig. 27). As kr_0 increases (the wave-length of the waves beings to be small compared with the radius of the peninsula), the inflow of the diffracted waves to the leeward waters becomes so small that the diffracted waves do not advance along the coast of the peninsula but depart from the coast to the outer sea. These diffracted waves cause the extension of the high amplitude region as a result of the superposition of weak reflected waves which are emitted from the leeward root (refer to Fig. 27). For the weak reflected waves lastly stated, the mechanism of generation of the waves is proposed to be a direct diffraction of the incident waves on the leeward root instead of the inflow along the coast of the peninsula (see Fig. 28).

6. Supplementary Note on Generation of Standing Waves

In order to further verify the existence of the standing waves along the coast of the semi-circular peninsula, the calculated results[2] for the waves around the semi-circular peninsula in which the incident waves

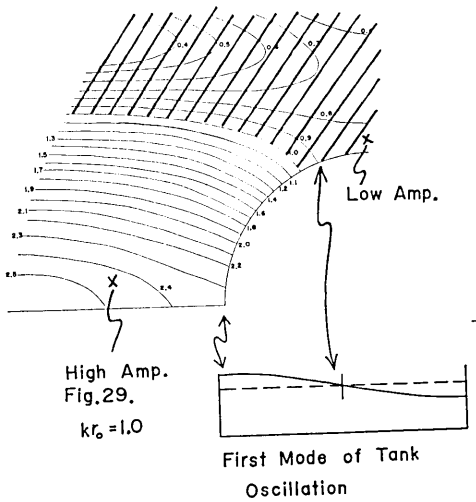

Fig. 29. Correspondence of the water motion in a rectangular tank and that around the peninsula in the case of the normal incidence of the wave with kr_0=1.0.

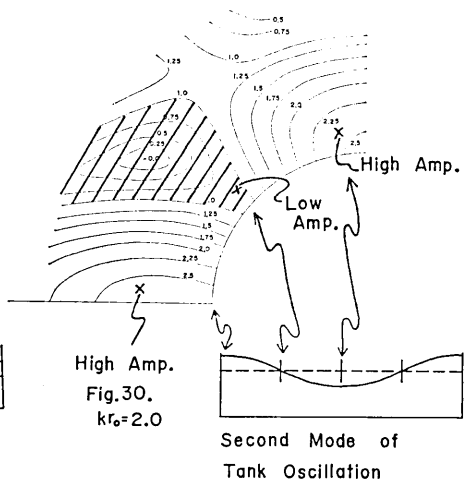

Fig. 30. Correspondence of the water motion in a rectangular tank and that around the peninsula in the case of the normal incidence of the wave with kr_0= 2.0.

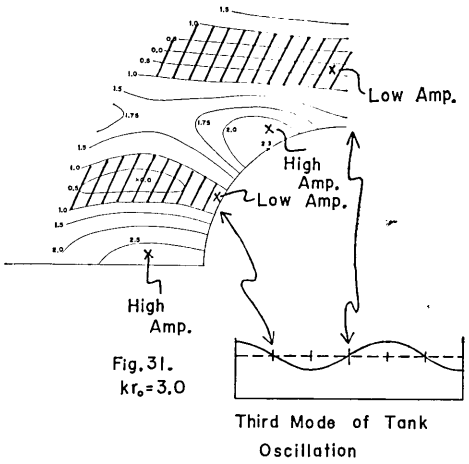

Fig. 31. Correspondence of the water motion in a rectangular tank and that around the peninsula in the case of the right-angled incidence of the wave with $kr_0=3.0$.

invade the straight coast perpendicularly are very useful. The figures relevant to the variations of amplitude in the work of reference number 2 (Figs. 2, 4 and 6 in the above study[2]), are reproduced in Figs. 29, 30 and 31 with a few supplementary figures. In the above figures (Figs. 29 to 31), the shaded regions denote those of small amplitude (below 1.0). In a way similar to that described in Fig. 6, the identifications of the above-mentioned parts of low amplitude and the nodes of the water tank oscillation are also carried out in these figures, where the length of the water tank is taken equal to that of the coast of the semi-circular peninsula. From these figures, we may arrive at the conclusion that, when a train of periodic waves invades a semi-circular peninsula, the standing waves are produced along the coast of the peninsula.

---

51. 半円型の半島に斜に入射した長波

地震研究所　桃　井　高　夫

本論文においては周期的な長波が半円型の半島に斜に入射したとき（入射角は 45 度にとられている）半島のまわりでおこされる長波の有様が論じられている．得られた結果のうちで最も著しいのは半島のまわりで定常波が発生することである．